

The 1D interacting Bose gas in a hard wall box

M.T. Batchelor[†], X.W. Guan[†], N. Oelkers[†] and C. Lee[‡]

[†] Department of Theoretical Physics, Research School of Physical Sciences and Engineering, and Department of Mathematics, Mathematical Sciences Institute, The Australian National University, Canberra ACT 0200, Australia

[‡] Nonlinear Physics Centre, Research School of Physical Sciences and Engineering, and ARC Centre of Excellence for Quantum-Atom Optics, The Australian National University, Canberra ACT 0200, Australia

Abstract. We consider the integrable one-dimensional δ -function interacting Bose gas in a hard wall box which is exactly solved via the coordinate Bethe Ansatz. The ground state energy, including the surface energy, is derived from the Lieb-Liniger type integral equations. The leading and correction terms are obtained in the weak coupling and strong coupling regimes from both the discrete Bethe equations and the integral equations. This allows the investigation of both finite-size and boundary effects in the integrable model. We also study the Luttinger liquid behaviour by calculating Luttinger parameters and correlations. The hard wall boundary conditions are seen to have a strong effect on the ground state energy and phase correlations in the weak coupling regime. Enhancement of the local two-body correlations is shown by application of the Hellmann-Feynman theorem.

PACS numbers: 05.30.-d, 67.40.Db, 05.30.Jp

1. Introduction

Quantum Bose and Fermi gases of ultracold atoms continue to attract considerable interest since the experimental realization of atomic Bose-Einstein condensates (BEC) [1, 2, 3, 4] and the pair condensation of fermionic atoms [5, 6, 7]. Particular attention has been paid to one-dimensional (1D) Bose gases, which are seen to exhibit the rich and novel effects of quantum many-body systems [8, 9, 10, 11, 12, 13, 14, 15]. As a consequence, there has been a revival of interest in the exactly solved 1D model of interacting bosons. It is well known that the δ -function interacting Bose gas is integrable [16, 17] and can be realized via short-range interactions with an effective coupling constant g_{1D} [9]. This constant is determined through an effective 1D scattering length $a_{1D} \approx a_{\perp}^2/a$, where a_{\perp} is the characteristic length along the transverse direction and a is the 3D scattering length. The ratio of the average interaction energy to the kinetic energy, $\gamma = \frac{mg_{1D}}{\hbar^2 n}$, is used to characterize the different physical regimes of the 1D quantum gas. Here m is the atomic mass and n is the boson number density. In the weak coupling regime, i.e., $\gamma \ll 1$, the wave functions of the bosons are coherent. In this regime, the density fluctuations are suppressed and the phase correlations decay algebraically at low temperatures. Thus the 1D Bose gas can undergo a quasi BEC. However, in the opposite limit, i.e., the Tonks-Girardeau limit $\gamma \gg 1$, the bosons behave like impenetrable hard core particles, the so called Tonks-Girardeau gas [18]. In this regime the single-particle wave functions become decoherent and the system acquires fermionic properties.

The 1D Bose gas is realized experimentally by tightly confining the atomic cloud in two (radial) dimensions and weakly confining it along the axial direction. The motion along the radial direction is then frozen to zero point oscillations [19, 20, 21, 22, 23], making the gas effectively one-dimensional. Anisotropic trapping along the radial and axial directions can form either a 2D optical lattice or 1D tubes. There have been two types of 1D quantum gases, the lattice Bose gas [19, 20, 21] and the continuum Bose gas confined in a harmonic potential along the axial direction [22] (see figure 1). From a theoretical point of view, the former is usually described by the Bose-Hubbard model while the latter is described by the 1D interacting Bose gas. The Bose-Hubbard model is not integrable, except for a special case [24], which corresponds to two sites. On the other hand, the trapping potential along the axial direction breaks the integrability of the 1D Bose gas. However, the long-wavelength properties of the 1D Bose gas and the Bose-Hubbard model can be described by a Luttinger liquid, owing to the universality of the low energy excitations, i.e., gapless excitations with a linear low-energy excitation spectrum and power-law decay in the correlations [25].

The exactly solved 1D interacting Bose gas has been extensively studied [26, 27, 28, 29, 17, 30, 31, 32, 33, 34]. The ground state energy and low energy excitations [16, 35], thermodynamic behaviour [36], finite-size effects [37], correlation functions [27, 38] and Luttinger liquid behaviour [39, 40, 41] have been investigated via various methods. The signature of the 1D Bose gas is strongly influenced by the interaction strength and the

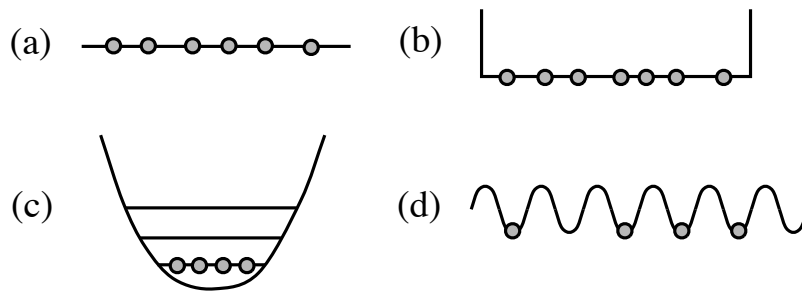


Figure 1. Schematic diagrams of different models used to describe experiments on quasi-1D bosons with contact interaction: (a) Bosons on a line with periodic boundary conditions (no potential) – exactly solved via Bethe Ansatz [16]. (b) Bosons confined to a hard-wall box – also exactly solved via Bethe Ansatz (this paper). Under certain conditions the hard walls can mimic a trapping potential. (c) Bosons confined by a harmonic trap potential – not exactly solved, but closer to experimental conditions. d) Lattice version realized by, e.g., experiments with optical lattices. The corresponding Bose-Hubbard type model is in general not integrable.

external trapping potential. The effects of spatial inhomogeneity and finite temperature are other considerations to be taken into account under experimental conditions. To this end, several approximation schemes have been adopted to describe the main features of the 1D trapped Bose gas. In particular, the local density approximation [11, 42, 43, 44] is widely used for calculating the density profiles of bosons and fermions in harmonic traps.

Now for a finite number of bosons and finite system size, boundary effects are expected to be pronounced at low temperature [45, 46, 47]. Indeed, significantly different quantum effects should be exhibited by a finite number of bosons confined in a finite hard wall box. For example, in the weak coupling regime, macroscopic states lie on the zero point oscillations as if the system undergoes BEC. The density expectation value exhibits Friedel oscillations and the correlation decay is slower than in the periodic case, due to the enhancement of the density and phase stiffness. The boundary conditions also have an effect on the phase correlations near the boundaries. The ground state of the 1D interacting Bose gas with hard wall boundary conditions has no momentum pairing (with a $-k$ for each k) compared to the period case, because of the missing translational symmetry. The hard wall boundary conditions have been experimentally realized by square potentials with very high barriers [48]. Most recently, BEC have been produced in a novel optical box trap [49], in which atom numbers are as small as 5×10^2 . More experiments in this direction can be anticipated [50, 51]. These are our motivations for studying the ground state properties of the 1D interacting Bose gas confined in a hard wall box.

The 1D interacting Bose gas with hard wall boundaries was solved by Gaudin in the early 1970's [52]. Gaudin calculated the surface energy via the Bethe Ansatz solution in the thermodynamic limit. Very recently, this model was studied via Haldane's harmonic

liquid theory [47, 40], which describes the long wave-length properties of the 1D fluid in terms of the density and phase fluctuations. The correlation functions of the Tonks-Girardeau gas have also been studied with hard wall boundary conditions [53].

The paper is organized as follows. In Section 2, we present the Bethe Ansatz wave functions and Bethe equations for the 1D interacting Bose gas with hard wall boundary conditions. Details of the Bethe Ansatz solution are given in Appendix A. In Section 3, we derive the ground state energy via asymptotic roots of the Bethe equations in the strong and weak coupling limits. We derive the surface energy through the continuum integral equations in Section 4. In Section 5, we calculate the ground state energy in the strong and weak coupling limits using Wadati's power series expansion method [31, 54, 55]. A discussion of the connection between the 1D Bose gas trapped by an harmonic potential and the exactly solved model is given in Section 6. The low-energy properties are discussed in Section 7, with concluding remarks given in section 8.

2. The Bethe Ansatz solution

The 1D quantum gas of N bosons with δ -function interaction in a hard wall box of length L is described by the Hamiltonian

$$\mathcal{H} = -\frac{\hbar^2}{2m} \sum_{i=1}^N \frac{\partial^2}{\partial x_i^2} + g_{1D} \sum_{1 \leq i < j \leq N} \delta(x_i - x_j) \quad (1)$$

where the hard walls are defined via the boundary conditions [52]

$$\Psi(x_1 = 0, x_2, \dots, x_N) = 0, \quad \Psi(x_1, x_2, \dots, x_N = L) = 0. \quad (2)$$

Here $g_{1D} = \hbar^2 c / m$ is an effective 1D coupling constant with scattering strength c . The wavefunction Ψ must be totally symmetric in all its arguments, as required for a bosonic system.

For harmonic trapping along the axial direction, the scattering strength is given by $c = \frac{2}{|a_{1D}|}$. The trapping potential should be added to the Hamiltonian (1) as an external field. However, harmonic potentials appear to break the integrability of the model. Fortunately the integrability of the model is preserved by the hard wall boundary conditions [52]. This provides us with an opportunity to study the signature of the 1D Bose gas in a hard wall box in an exact fashion. For simplicity, we set $\hbar = 2m = 1$ in the following.

The explicit solution of the model via the coordinate Bethe Ansatz is described in Appendix A. The wavefunction is given by

$$\Psi_{\{\epsilon_i k_i\}}(x_1, \dots, x_N) = \sum_{\epsilon_1, \dots, \epsilon_N} \sum_P \epsilon_1 \cdots \epsilon_N A(\epsilon_1 k_{P1} \cdots \epsilon_N k_{PN}) e^{i(\epsilon_1 k_{P1} x_1 + \cdots + \epsilon_N k_{PN} x_N)} \quad (3)$$

where the sum extends over all $N!$ permutations P and all signs $\epsilon_i = \pm$ (see Appendix A). The wavefunction is valid in the domain $0 \leq x_1 < \dots < x_N \leq L$ and can be continued

via symmetry in all coordinates x_i . The wavefunction coefficients $A(\epsilon_1 k_{P_{x_1}} \cdots \epsilon_N k_{P_{x_N}})$ are determined by the Bethe roots, or wave numbers, k_i via

$$A(\epsilon_1 k_{P_1} \cdots \epsilon_N k_{P_N}) = (-)^P \prod_{i=1}^{N-1} \prod_{j>i}^N (\epsilon_i k_{P_i} - \epsilon_j k_{P_j} + ic)(\epsilon_i k_{P_i} + \epsilon_j k_{P_j} - ic). \quad (4)$$

In the above equation $(-)^P$ denotes a (\pm) sign factor associated with even/odd permutations. The wave numbers satisfy the Bethe equations

$$e^{i2k_j L} = - \prod_{\ell=1}^N \frac{(k_j - k_\ell + ic)(k_j + k_\ell + ic)}{(k_j - k_\ell - ic)(k_j + k_\ell - ic)} \quad \forall j = 1, \dots, N. \quad (5)$$

The energy eigenvalues are as usual given by

$$E = \sum_{j=1}^N k_j^2. \quad (6)$$

Like the periodic boundary condition case [27], the Bethe roots k_i are known to be real for repulsive interactions ($c > 0$), but they may become complex for attractive interactions ($c < 0$). Here we consider the repulsive regime. Free bosons are recovered for $c = 0$, i.e., $k = \pi n/L, n \in \mathbb{N}$ (see Appendix A).

3. Asymptotic solutions to the Bethe equations

In contrast with periodic boundary conditions, the ground state no longer contains \pm momentum pairs due to the reflection of quasi momenta at the boundaries. As a result the total quasi momentum $\sum_{j=1}^N k_j$ is not conserved in this case. We first examine the asymptotic solutions of the Bethe equations (5) in the strong and weak coupling limits.

3.1. Tonks-Girardeau regime

It is well known that in the strong coupling regime, i.e., $\gamma \gg 1$, the 1D Bose gas with repulsive interaction behaves like a gas of weakly interacting fermions [51]. In the limiting case $c = \infty$ the exact solution for periodic boundary conditions and harmonic trapping has been given for impenetrable bosons [18, 14]. In the hard wall setting the fermionic behaviour can be seen from the ground state energy. Define the variables $z_j = Lk_j/N$ and $\gamma = Lc/N$. Then for $\gamma \gg 1/N$ the Bethe equations (5) can be written in the asymptotic form

$$\begin{aligned} \exp(i2Nz_j) \approx & 1 - 2 \sum_{\ell=1}^N \left\{ \frac{(z_j - z_\ell)^2}{\gamma^2} + \frac{(z_j + z_\ell)^2}{\gamma^2} \right\} - 4 \sum_{\ell=1}^{N-1} \sum_{\ell' < \ell}^N \frac{(z_j - z_\ell)(z_j + z_{\ell'})}{\gamma} \\ & - 2i \sum_{\ell=1}^N \left\{ \frac{(z_j - z_\ell)}{\gamma} + \frac{(z_j + z_\ell)}{\gamma} \right\} \quad \forall j = 1, \dots, N \end{aligned} \quad (7)$$

in which the summations exclude $\ell = j$ and $\ell' = j$. Here we restrict the solutions to $z_j > 0$. The asymptotic Bethe roots

$$z_j \approx \frac{\pi j}{N} \left(1 + \frac{2(N-1)}{N\gamma} \right)^{-1} \quad \forall j = 1, \dots, N \quad (8)$$

for the ground state energy follow from the condition that the eqns (7) be consistent. It follows that in this limit the ground state energy per particle is given by

$$\frac{E}{N} \approx \frac{\pi^2}{6L^2}(N+1)(2N+1) \left(1 + \frac{2(N-1)}{Lc}\right)^{-2}. \quad (9)$$

We emphasize that these asymptotic solutions are very accurate for the Tonks-Girardeau regime. We will compare the ground state energy (9) with numerical solutions of the continuum integral equation, which is the hard-wall analogue of the Lieb-Liniger integral equation, in Section 4. The explicit form for the wave numbers k_j also allows an in principle calculation of the asymptotic correlation functions directly from the wave function (3). Switching back to real physical units, the ground state energy per particle (9) can also be written as

$$\frac{E}{N} \approx \frac{\hbar^2 n^2}{2m} \left(e_0(\gamma) + \frac{1}{N} e_f(\gamma) \right). \quad (10)$$

Here the bulk energy $e_0(\gamma)$ and the surface energy $e_f(\gamma)$ are given by

$$e_0(\gamma) = \frac{\pi^2}{3} \left(1 + \frac{2}{\gamma}\right)^{-2} \quad (11)$$

$$e_f(\gamma) = \frac{\pi^2}{2} \left(1 + \frac{2}{\gamma}\right)^{-2}. \quad (12)$$

A useful quantity is the 1D temperature $T_{1D} = \frac{2E}{Nk_B}$, which is just the ground state energy in different units [22]. We plot T_{1D} obtained from (10) as a function of the interaction strength γ in figure 2 for a gas of $N = 37$ bosons confined in boxes of length $L = 35.25 \mu\text{m}$ and $L = 32.61 \mu\text{m}$. These are the same parameters as in Figure 3 of Ref [22]. The dashed horizontal lines are the corresponding values of T_{1D} in the Tonks-Girardeau limit. We remark that for hard wall boundary conditions, the particle density distribution is rather flat and homogeneous. It can be seen that T_{1D} increases rapidly as γ increases in the weak coupling regime. It then slowly approaches the Tonks-Girardeau energy as γ tends to infinity. In an actual experiment, the length of the atomic cloud varies with the interaction strength. In that case the T_{1D} will increase smoothly as γ increases. Most significantly, T_{1D} is sensitive to the length of the hard wall box. The smaller the length of the box, the larger the ‘quasi-momentum’ of the particles. We note also that the surface energy is positive. In the thermodynamic limit, the ground state energy for periodic boundary conditions is proportional to the linear density n . Therefore, in the thermodynamic limit, the ground state energy per particle of the Bose gas in a hard wall box can be considered as an excited state of a Bose gas with $2N$ particles in a periodic box of length $2L$ [52]. We will study the ground state properties for the hard wall box further in Section 4.

3.2. Weak coupling regime

The ground state properties in the weak coupling limit are both subtle and interesting. So far it has proved difficult to reach the weak coupling regime via anisotropic trapping

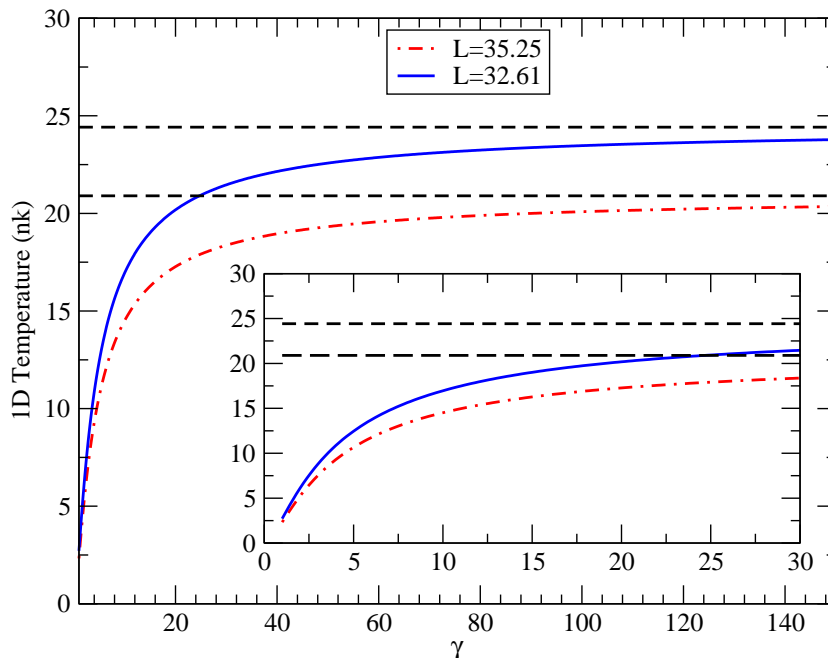


Figure 2. The 1D temperature T_{1D} obtained from the asymptotic result (10) versus interaction strength γ for $N = 37$ ^{87}Rb atoms confined in 1D boxes of length $L = 35.25\mu\text{m}$ and $L = 32.61\mu\text{m}$. The asymptotic result (10) is valid for a wide range of interaction, i.e. $\gamma \gg 1/N$. The horizontal dashed lines are the corresponding temperatures in the Tonks-Girardeau limit. The inset shows the 1D temperatures in the regime $1 < \gamma < 30$.

in experiments [22] and it is necessary to sharply define the criterion for weak coupling [41, 43]. In the experiment, the 1D regime is reached if the radial zero point oscillation length $l_0 = \sqrt{\hbar/(m\omega_\perp)}$ is much smaller than the axial correlation length $l_c = \hbar/\sqrt{m\mu}$, where ω_\perp is the frequency of the radial trap and μ is the chemical potential of the 1D system, thus the condition is $\mu \ll \hbar\omega_\perp$ for the 1D trapped system. In general, $\gamma \ll 1$ at zero temperature is referred to as the weak coupling regime. The Thomas-Fermi regime is usually reached for $\mu \gg \hbar\omega$, where ω is the axial oscillation frequency for the harmonic trap. In this regime the kinetic energy term can be neglected and the system has a parabolic density distribution profile [11], referred to as the Thomas-Fermi BEC. However, in the regime $\mu \ll \hbar\omega$ the system is considered to have a macroscopic occupation in the ground state of the trap with a Gaussian density profile [41].

For the hard wall boundary conditions, the leading terms in the ground state energy can be obtained through asymptotic solutions of the Bethe equations (5) in analogy with the periodic case [34]. Here the wave numbers k_j for the ground state satisfy the algebraic equations

$$k_j = \frac{\pi}{L} + \frac{c}{L} \sum_{\substack{\ell=1 \\ \ell \neq j}}^N \left(\frac{1}{k_j - k_\ell} + \frac{1}{k_j + k_\ell} \right) \quad \forall j = 1, \dots, N. \quad (13)$$

Algebraic equations for periodic boundary conditions have arisen in a number of different contexts [34], most notably in the integrable BCS pairing models [56]. The roots of such equations also describe the equilibrium positions of potentials in Calogero systems associated with Lie algebras [57].

The solutions of (13) give the ground state energy

$$\frac{E}{N} \approx \frac{\pi^2}{L^2} + \frac{3(N-1)c}{2L}. \quad (14)$$

This is quite different from the periodic boundary case, for which the leading term in the ground state energy per particle is $\frac{E}{N} \approx (N-1)c/L$. Here, due to the reflections at the boundaries, the ground state energy for hard wall boundary conditions is larger than the energy for periodic boundary conditions. For the integrable 1D Bose gas with periodic boundary conditions, the ground state energy per particle is known to be given by $\frac{E}{N} \approx \frac{\hbar^2 n^2}{2m} e_0(\gamma)$ with $e_0(\gamma) \simeq \gamma \left(1 - \frac{4}{3\pi} \sqrt{\gamma}\right)$ [16, 28, 31]. We argue that this result holds in the regime $1/N^2 \ll \gamma \ll 1$. The leading term of the ground state energy per particle for periodic boundary conditions, i.e. $\frac{E}{N} \approx \frac{\hbar^2 n^2}{2m} \gamma$ holds in the mean-field regime, i.e., $\gamma \ll 1/N^2$, for which the correction term is proportional to γ^2 rather than $\gamma^{3/2}$. This discrepancy is not totally unexpected, as the Lieb-Liniger integral equation is only valid up to terms of order $1/L$. If the interaction energy is much smaller than the scale of $1/L$, i.e., if $\gamma \ll 1/N^2$, results derived from the Lieb-Liniger integral equation are no longer valid in this very weak coupling regime. On the other hand, in the regime $\gamma \gg 1/N^2$ the zero point oscillation kinetic energy is much smaller than the interaction energy and is thus negligible – it is here that one can derive the ground state energy asymptotically from the continuum integral equation. Finite-size discrepancies between the discrete and integral equation approaches have also been noted in Ref. [58].

4. The surface energy

Taking the logarithm on both sides of the Bethe equations (5) gives

$$\bar{k}_j L = \pi m_j - \sum_{\ell=1}^N \left\{ \arctan \frac{\bar{k}_j - \bar{k}_\ell}{c} + \arctan \frac{\bar{k}_j + \bar{k}_\ell}{c} \right\} \quad (15)$$

where $j = 1, \dots, N$ and m_j are ordered positive integers, i.e., $1 \leq m_1 \leq \dots \leq m_N$. Here for later convenience we have denoted the Bethe roots by \bar{k} . Our calculation takes advantage of the fact that in the thermodynamic limit, the ground state energy of the N boson system in a box of length L is equivalent to one half the energy of $2N$ bosons with length $2L$ and periodic boundary conditions, as pointed out by [52]. It is thus convenient to derive the surface energy from a periodic system of $2N$ bosons with a length $2L$, for which the Bethe equations are [16]‡

$$k_j L = 2\pi I_j - \sum_{\ell=1}^N \left\{ \arctan \frac{k_j - k_\ell}{c} + \arctan \frac{k_j + k_\ell}{c} \right\} \quad (16)$$

‡ Of course, one may also obtain the same free energy by treating the Bethe equations (15) directly, see, e.g., Ref. [59].

for $k_j > 0$ and I_j are half-odd integers. We now introduce the notation $k_{-j} = -k_j$ and $I_{-j} = -I_j$. The difference between \bar{k}_j and k_j can thus be written as

$$(\bar{k}_j - k_j)L = \pi\epsilon_j - \sum_{\ell=-N}^N \left\{ \arctan \frac{\bar{k}_j - \bar{k}_\ell}{c} - \arctan \frac{k_j - k_\ell}{c} \right\} \quad (17)$$

where $j = -N, \dots, N$ and ϵ_j is a sign factor.

The surface energy is given by

$$E_f = \frac{1}{2} \sum_{j=-N}^N (\bar{k}_j^2 - k_j^2). \quad (18)$$

Using $\bar{k}_j - k_j < \pi/L$ and taking the Taylor expansion of equations (17) at $\bar{k}_j = k_j + \Delta k_j$ gives

$$\Delta k_j L = \pi\epsilon_j - \sum_{\ell=-N}^N \frac{c(\Delta k_j - \Delta k_\ell)}{c^2 + (k_j - k_\ell)^2}. \quad (19)$$

It follows that

$$\Delta k_j \left(1 + \frac{1}{L} \sum_{\ell=-N}^N \frac{c}{c^2 + (k_j - k_\ell)^2} \right) = \frac{1}{L} \left(\pi\epsilon_j + \sum_{\ell=-N}^N \frac{c\Delta k_\ell}{c^2 + (k_j - k_\ell)^2} \right). \quad (20)$$

Let us define $k_{j+1} - k_j = \frac{1}{2Lf(k_j)}$, where $f(k)$ is the distribution function [16], then the Bethe equations (16) become

$$2\pi f(k) = 1 + 2c \int_{-B}^B \frac{f(k')}{c^2 + (k - k')^2} dk'. \quad (21)$$

Here we use the density $n = \frac{2N}{2L}$ and define the cut-off momentum B . Subsequently, equation (19) becomes

$$\Delta k f(k) = \frac{1}{2L}\epsilon(k) + \frac{c}{\pi} \int_{-B}^B \frac{\Delta k' f(k')}{c^2 + (k - k')^2} dk'. \quad (22)$$

Here $\epsilon(k) = \text{sgn}(k)$. Further defining $f_f(k) = L\Delta k f(k)$, the surface energy is given by

$$E_f = \int_{-B}^B k f_f(k) dk \quad (23)$$

where $f_f(k)$ satisfies the integral equation

$$f_f(k) = \frac{1}{2}\epsilon(k) + \frac{c}{\pi} \int_{-B}^B \frac{f_f(k')}{c^2 + (k - k')^2} dk'. \quad (24)$$

After the same rescaling as introduced in Ref. [16], i.e., $k = Bx$, $c = B\lambda$, $f(Bx) = g(x)$, we find the ground state energy per particle to be of the form (10). The bulk and surface energies are given by

$$e_0(\gamma) = \frac{\gamma^3}{\lambda^3} \int_{-1}^1 g_0(x) x^2 dx \quad (25)$$

$$e_f(\gamma) = \frac{\gamma^2}{\lambda^2} \int_{-1}^1 g_f(x) x dx \quad (26)$$

where

$$g_0(x) = \frac{1}{2\pi} + \frac{\lambda}{\pi} \int_{-1}^1 \frac{g_0(y)}{\lambda^2 + (x-y)^2} dy \quad (27)$$

$$g_f(x) = \frac{1}{2}\epsilon(x) + \frac{\lambda}{\pi} \int_{-1}^1 \frac{g_f(y)}{\lambda^2 + (x-y)^2} dy \quad (28)$$

with the cut-off condition

$$\gamma \int_{-1}^1 g_0(x) dx = \lambda. \quad (29)$$

There are various methods which can be used to solve the above equations (27) and (28). In the next section we derive analytic results from these equations in the strong and weak coupling limits.

5. Application of Wadati's power series expansion method

As remarked in references [52, 55], the Lieb-Liniger integral equation is closely related to the Love equation for the problem of a circular plate condensator [60]. One can obtain a series expansion for the ground state energy from the integral equation [31]. This method has also been applied to the Yang-Yang integral equations for the thermodynamics [54] and to the Gaudin integral equation for the attractive δ -function interacting Fermi gas [55]. For the Bose gas with hard walls, Gaudin [52] found the leading surface energy term in the weakly interacting limit. In this section, we apply the Wadati method to obtain the leading terms in the ground state energy from the integral equations (27) and (28).

5.1. Tonks-Girardeau regime

In the strong coupling regime the bulk part of the ground state energy per particle is given by [16, 31, 34]

$$e_0(\gamma) \approx \frac{\pi^2}{3} \left(\frac{\gamma}{\gamma+2} \right)^2 \quad (30)$$

which agrees with the asymptotic result (11). Calculating the first two terms in the expansion

$$g_f(x) \approx a_0 + a_1 x^2 \quad (31)$$

for the distribution function (28), we find

$$a_0 = \frac{\epsilon(x)(\gamma+2)}{2\gamma} \left[1 - \frac{2x^2}{3\gamma(\gamma+2)^2} \right] \quad (32)$$

$$a_1 = \frac{\epsilon(x)\pi^2}{\gamma(\gamma+2)}. \quad (33)$$

This leads to the surface energy

$$e_f \approx \frac{\pi^2}{2} \left(\frac{\gamma}{\gamma+2} \right) \left(1 + \frac{\pi^2(\gamma-2)}{3\gamma(\gamma+2)} - \frac{2\pi^2}{3\gamma^2(\gamma+2)} \right). \quad (34)$$

We see that the constant term in the surface energy (34) is the same as in (12), but the leading correction term differs. Again this is because the continuum integral equation derived from the Bethe equations is only valid for terms of order up to $1/L$.

5.2. Weak coupling regime

In this regime the leading terms of the distribution function are found to be

$$g_f(x) \approx \frac{\epsilon(x)}{\sqrt{\gamma}} \sqrt{1-x^2}. \quad (35)$$

The surface energy $e_f \approx \frac{8}{3}\sqrt{\gamma}$ follows from equation (28). Here we keep only the leading term, as for a large number of particles, the contribution from other terms is negligible. The ground state energy per particle in the regime $1/N^2 \ll \gamma \ll 1$ is again of the form (10) where the leading bulk and surface energy terms are

$$e_0(\gamma) \approx \gamma \left(1 - \frac{4}{3\pi} \sqrt{\gamma}\right) \quad (36)$$

$$e_f(\gamma) \approx \frac{8\sqrt{\gamma}}{3}. \quad (37)$$

So far we have derived some analytic results for the ground state energy of the interacting 1D Bose gas with hard wall boundary conditions. One may also perform direct numerical calculations using the integral equations (27) and (28), as originally done in the bulk [16]. In doing this we see that the ground state energy (10), with (11) and (12), is consistent with the result obtained from the the integral equations (27) and (28) for $\gamma > 1$, with best agreement found for $\gamma > 5$ (see figure 3). A comparison between the analytic result and numerical calculation for weak coupling is presented in Figure 4. A discrepancy between the numerical and analytic results is evident for weak coupling. This implies that the next leading term in the surface energy (37) is necessary. As expected, there is a difference between the finite-size results and the limiting curve obtained in the thermodynamic limit.

6. Comparison with the 1D Bose gas trapped by harmonic potentials

The experimental realization of the Tonks-Girardeau gas trapped in harmonic potentials has involved the measurement of momentum distribution profiles [20, 21], the ground state energy [22] and collective oscillations [23]. To model the experiments more closely it is desirable to take into account the ‘soft’ boundaries of the harmonic potential rather than the commonly used ‘hard’ boundaries of a box. Unfortunately the axial trapping potential breaks the homogeneity of the integrable model. However, if the density varies smoothly in a small interval the systems under consideration can be thought of as a uniform Bose gas in each small interval [11, 41, 43]. This quasiclassical approach is called the *local density approximation* and is used to study the density distribution profile in cases where the chemical potential is much larger than the level spacing $\hbar\omega$ in the 1D direction. For the equilibrium state the chemical potential of the system in a harmonic trap can be taken to be constant.

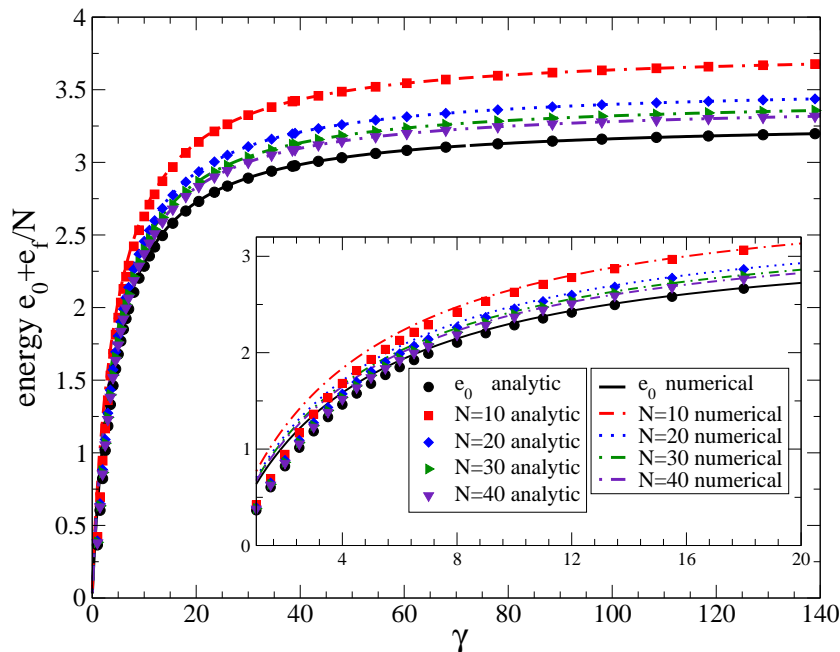


Figure 3. The ground state energy $e_0 + \frac{1}{N}e_f$ versus the interaction strength γ for $N = 10, 20, 30, 40$ particles. For each size there is a comparison between the numerical solution of the integral equations (27) and (28) and the analytic expression for strong coupling (10), with (11) and (12), derived from the discrete Bethe equations (5). A generally good agreement between the numerical and analytic results is visible. The lowest curve is obtained in the thermodynamic limit.

Applying the local density approximation to the 1D Bose gas with periodic boundary conditions at zero temperature, we have

$$\mu(n(z)) + V(z) = \mu_0 \quad (38)$$

where $\mu(n(z))$ is the local chemical potential of the uniform system and $V(z) = \frac{1}{2}m\omega^2 z^2$ is the local trapping potential. We make the Ansatz

$$\begin{cases} \mu(n(z)) + V(z) = \mu_0, & \text{for } |z| \leq R \\ n(z) = 0, & \text{for } |z| > R \end{cases} \quad (39)$$

where R is the atomic cloud radius given by $R = \sqrt{\frac{2\mu_0}{m\omega^2}}$. The density profile of the system can be obtained by using the normalization condition

$$\int_{-R}^R n(z) dz = N. \quad (40)$$

With help of the analytical expressions for the ground state energy of the interacting Bose gas it is now straightforward to derive the density profiles in the Thomas-Fermi and Tonks-Girardeau regimes.

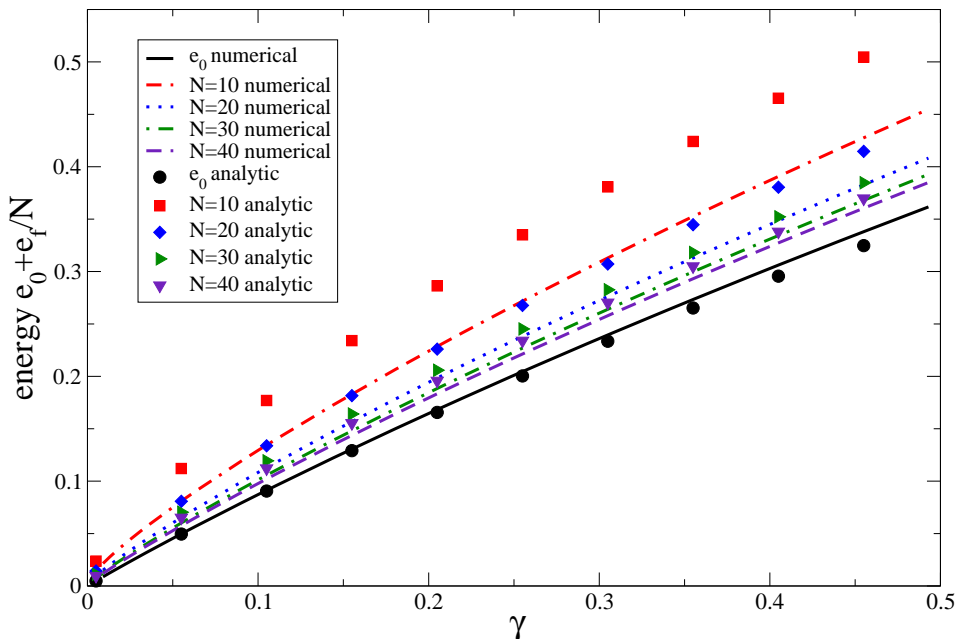


Figure 4. Ground state energy $e_0 + \frac{1}{N}e_f$ in the weak coupling regime versus the interaction strength γ for $N = 10, 20, 30, 40$. For each size there is a comparison between the numerical result evaluated from the integral equations (27) and (28) and the analytic expressions for weak coupling, (36) and (37). A slight discrepancy between the numerical and analytic results appears for weak coupling. This discrepancy becomes small if the particle number is very large. The analytic expressions are expected to hold in the region $1/N^2 \ll \gamma \ll 1$.

For the Thomas-Fermi regime, the energy per particle is given by $E_0 = \frac{\hbar^2}{2m}n(z)c$ and thus

$$n(z) = n_{\text{TF}}^0 \left(1 - \frac{z^2}{R_{\text{TF}}^2} \right) \quad (41)$$

with central density and Thomas-Fermi radius

$$n_{\text{TF}}^0 = \left(\frac{9m^2\omega^2 N^2}{32c\hbar^2} \right)^{\frac{1}{3}}, \quad R_{\text{TF}} = \left(\frac{3N\hbar^2 c}{2m^2\omega^2} \right)^{\frac{1}{3}}. \quad (42)$$

Here $c = 2/|a_{1D}|$. The average energy per particle is given by

$$E_{\text{TF}} \approx \frac{1}{N} \int_{-R_{\text{TF}}}^{R_{\text{TF}}} n(z) E_0(n(z)) dz = \frac{1}{5} \left(\frac{9N^2\omega^2 \hbar^4 c^2}{4m} \right)^{\frac{1}{3}}. \quad (43)$$

In the Tonks-Girardeau limit, the local chemical potential is $\mu(n(z)) = \frac{\hbar^2\pi^2}{2m}n^2(z)$ and the density distribution is given by $n(z) = n_{\text{TG}}^0 \sqrt{1 - \frac{z^2}{R_{\text{TG}}^2}}$, with

$$n_{\text{TG}}^0 = \sqrt{\frac{2Nm\omega}{\pi^2\hbar}}, \quad R_{\text{TG}} = \sqrt{\frac{2\hbar N}{m\omega}}. \quad (44)$$

The average energy per particle in the Tonks-Girardeau limit is $E_{\text{TG}} \approx \frac{1}{4}\hbar N\omega$. The density profile has been studied in the whole regime [11]. The cloud size expands as the interaction strength increases. In the Tonks-Girardeau regime, the interaction-dependent radius is given approximately by

$$R \approx R_{\text{TG}} \left(1 - \frac{32}{9\pi^2} \frac{R_{\text{TG}} |a_{1\text{D}}|}{R_0^2} \right). \quad (45)$$

Indeed this would slow down the increasing of the average energy with increasing interaction strength in the weak coupling regime if we consider the length of the hard wall box varying with γ via the relation $L = 2R$. However, further refinements are necessary for finite systems, i.e., for a finite number of confined bosons.

In the previous sections we have discussed in detail the derivation of the ground state energy of the 1D interacting Bose gas confined in a hard wall box. This integrable system is much easier to treat theoretically than the system with harmonic trapping. The experimentally measured 1D energy has been compared with theoretical curves obtained using the local density approximation [22]. However, the theoretical predictions are not convincing for a number of reasons. First it is not clear if the quantity γ_{avg} presented in the Figures of Ref. [22] corresponds to the dimensionless interacting strength γ in the uniform Hamiltonian (1). Secondly, the interaction strength region measured, up to $\gamma_{\text{avg}} < 6$, may be too small to be sure that the Tonks-Girardeau regime has been reached. Our theoretical results indicate that finite-size effects induced from the number of particles, the system size and the boundary conditions are not negligible in the weak coupling and Tonks-Girardeau regimes.

There is some similarity between harmonic trapping and hard wall box confinement. For $\gamma = 0$, the kinetic zero point oscillation energy is $\frac{1}{4}\hbar\omega$ for axial harmonic trapping. If we confine the 1D Bose gas in a hard wall box of length $L = 2R_0$, where $R_0 = \sqrt{\frac{2\hbar}{m\omega}}$ is the characteristic length of the harmonic oscillator, the kinetic energy per particle is $\frac{\pi^2}{16}\hbar\omega$ for the hard wall boundary conditions, which is much larger than the kinetic zero point oscillation energy, for harmonic trapping. For the Tonks-Girardeau regime, if we confine the 1D Bose gas in a length $L = 2R_{\text{TG}}$, the 1D energy per particle is $\frac{\pi^2}{16}(\frac{1}{3} + \frac{1}{2N})N\hbar\omega$, which is almost the same as the average 1D energy $E_{\text{TG}} \approx \frac{1}{4}\hbar N\omega$ for harmonic trapping.

The boundary effects are more pronounced in the weak coupling limit. If one takes the same zero point kinetic energy and 1D ground state energy for the hard wall box as that for harmonic trapping, the size of the hard wall box for the $\gamma = 0$ and $\gamma = \infty$ limits should be $L_0 = \sqrt{\frac{2\hbar\pi^2}{m\omega}}$ and $L_{\text{TG}} = \sqrt{\frac{2\hbar N\pi^2}{m\omega}(\frac{1}{3} + \frac{1}{2N})}$, respectively. Recall that we plotted the 1D temperature as a function of the interaction strength for the hard wall boundary conditions with $L_{\text{TG}} = 32.61\mu\text{m}$ and $L = 2R_{\text{TG}} = 35.25\mu\text{m}$ in figure 2. These numerical values follow on inserting the physical parameters for ^{87}Rb atoms into the above results, with $N = 37$, $^{87}m = 0.1454 \times 10^{-24}$ and $\omega = 2\pi \times 27.5$. In this way figure 2 can be compared with the experimental data in Figures 3A and 4 of Ref [22]. As observed in Ref. [22], the radius R of the atomic cloud for harmonic trapping increases

rapidly with the interaction strength in the weak coupling regime, causing the average energy to increase rather slowly in comparison with the hard wall case.

7. Luttinger liquid behaviour

Many one-dimensional models behave like Tomonaga-Luttinger liquids due to the universality of the dispersion relation and correlation behaviour. The low energy properties are characterized by power-law decay in the correlation functions with gapless excitations. A universal description of the low-energy properties of one-dimensional interacting systems has been given in terms of harmonic liquid theory [25]. The 1D Bose and Fermi gases are included in this theory. The Luttinger liquid behaviour of the 1D Bose gas has recently been studied with hard wall boundary conditions [47]. It was found that the particle density exhibits Friedel oscillations with respect to the distance to the boundaries. The phase and density correlations are influenced by the hard wall boundary effects. Here we examine this behaviour in the context of the integrable model.

7.1. The Luttinger parameters

The harmonic liquid approach to the low energy excitations of the 1D Bose gas is described by the effective Hamiltonian [25, 40, 47]

$$H_{\text{eff}} = \frac{1}{2} \hbar v_s \int_0^L dx \left[\frac{\pi}{K} \Pi^2(x) + \frac{K}{\pi} (\partial\phi(x))^2 \right] \quad (46)$$

where $K = \sqrt{v_J/v_N}$, with $v_s = \sqrt{v_N v_J}$, is the Luttinger liquid parameter. Here v_J is the phase stiffness, v_N is the density stiffness and v_s is the sound velocity. For the long-wavelength density fluctuations the density $\rho(x) = \rho_0 + \Pi(x)$ has small deviations from the ground state density ρ_0 . The boson field operator is defined as $\Psi^\dagger(x) = \sqrt{\rho(x)} e^{-i\phi(x)}$, where $[\rho(x), e^{-i\phi(x')}] = \delta(x - x') e^{-i\phi(x)}$. The effective Hamiltonian (46) is reduced to the quantum hydrodynamic Hamiltonian [40, 47]

$$H_{\text{eff}} = \sum_{q>0} \hbar\omega(q) b^\dagger(q) b(q) + \frac{\hbar\pi v_s}{2LK} (N - N_0)^2 \quad (47)$$

with regard to the particle-hole excitation modes. Here $\omega(q) = v_s q$ for $q \ll \rho_0$ and the wave number is restricted to $q > 0$. N is the total number of particles in the system and N_0 is the number in the ground state, with $b^\dagger(q)$ the creation operator of elementary excitations. The low energy excitations are well described by the effective Hamiltonian (47) with Luttinger parameters v_s and K . We now study the effect of the hard walls on the Luttinger liquid parameters. The density stiffness and sound velocity can be derived from the ground state energy via the relations [35, 40]

$$v_N = \frac{L}{\pi\hbar} \left[\frac{\partial^2 E}{\partial N^2} \right], \quad v_s = \sqrt{\frac{L}{mn} \left[\frac{\partial^2 E}{\partial L^2} \right]}. \quad (48)$$

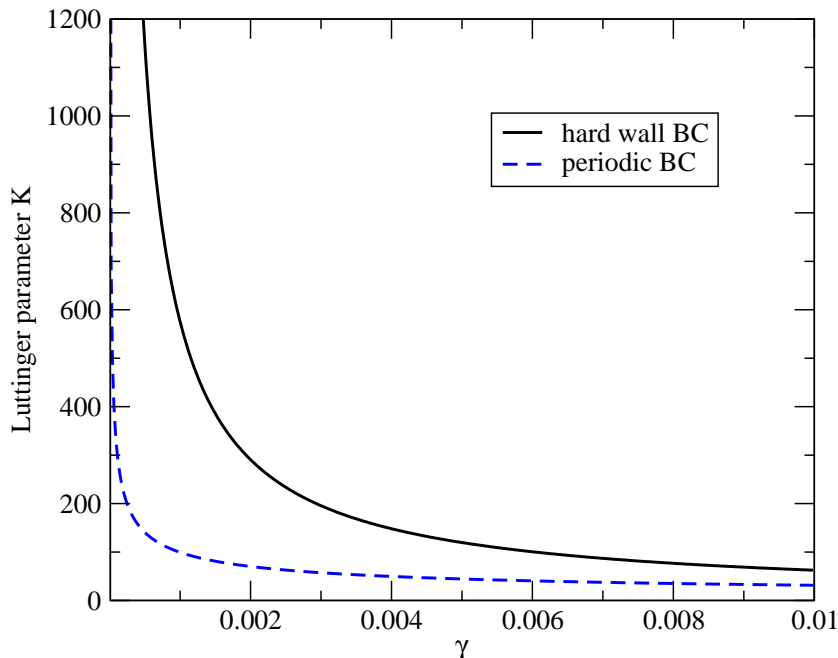


Figure 5. Plot of the Luttinger liquid parameter K as a function of the interaction strength γ for $N = 20$ bosons with hard wall boundaries (solid line) and periodic boundary conditions (dashed line).

Although the regime $\gamma \ll 1/N^2$ is difficult to achieve in experiments, the boundaries nevertheless have a significant effect on the Luttinger behaviour in this regime. Using the ground state energy (14), we have

$$v_N = \frac{3\gamma}{2\pi^2}v_F, \quad v_s = v_F \sqrt{3 \left(\frac{1}{N^2} + \frac{\gamma}{2\pi^2} \right)}. \quad (49)$$

Here the Fermi velocity $v_F = \hbar\pi n/m$. We see that the Luttinger liquid parameter $K \approx \frac{2\pi^2}{\sqrt{3\gamma}} \sqrt{\frac{1}{N^2} + \frac{\gamma}{2\pi^2}}$ tends to infinity for $\gamma \rightarrow 0$ at a faster rate than for periodic boundaries, for which $K \approx \pi/\sqrt{\gamma}$ [40] (see Figure 5). The enhancement of K for hard wall boundary conditions leads to a very slow decay of the phase correlation [40, 47]. The momentum distribution exponentially decays as $n(p) \sim p^{-\beta}$, where $\beta = 1 - \frac{1}{2K}$ [47]. The system behaves like a BEC in this regime.

In the Thomas-Fermi regime $1/N^2 \ll \gamma \ll 1$ we use the ground state energy in Section 5.2 to obtain the parameters

$$v_N = v_F \frac{\gamma}{\pi^2} \left(1 - \frac{\sqrt{\gamma}}{2\pi} + \frac{1}{N\sqrt{\gamma}} \right), \quad (50)$$

$$v_s = v_F \frac{\sqrt{\gamma}}{\pi} \left(1 - \frac{\sqrt{\gamma}}{2\pi} + \frac{5}{N\sqrt{\gamma}} \right), \quad (51)$$

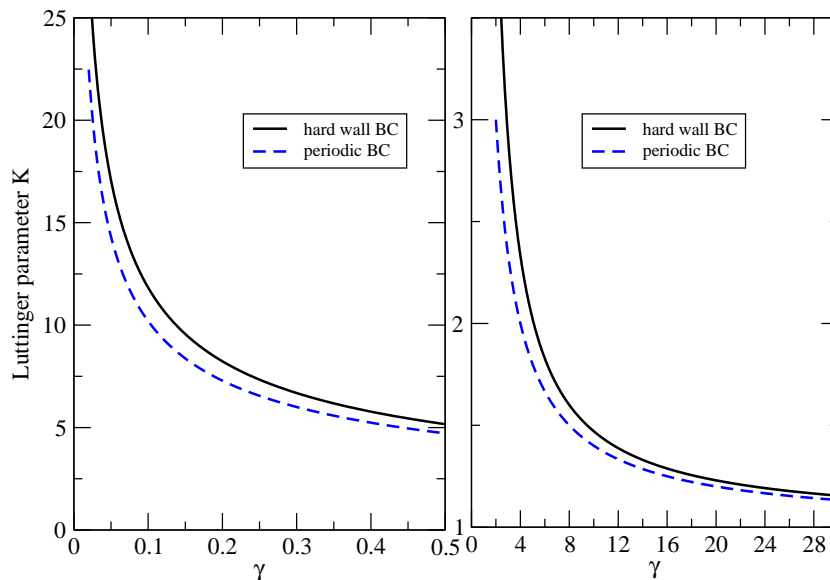


Figure 6. Plot of the Luttinger liquid parameter K versus the interaction strength γ for $N = 20$ bosons with hard wall boundaries (solid line) and periodic boundary conditions (dashed line) in (left) the Thomas-Fermi regime and (right) the strong coupling regime. In the Tonks-Girardeau limit K tends to the value $1 + \frac{1}{4N}$.

$$K = \frac{\pi}{\sqrt{\gamma}} \frac{\sqrt{1 - \frac{\sqrt{\gamma}}{2\pi} + \frac{5}{N\sqrt{\gamma}}}}{1 - \frac{\sqrt{\gamma}}{2\pi} + \frac{1}{N\sqrt{\gamma}}}. \quad (52)$$

In the strong coupling regime we use the result (9) to obtain

$$v_N = v_F \left(1 + \frac{2}{\gamma}\right)^{-4} \left[1 + \frac{1}{2N} \left(1 - \frac{4}{\gamma}\right)\right], \quad (53)$$

$$v_s = v_F \frac{\sqrt{1 + \frac{3}{2N}}}{\left(1 + \frac{2}{\gamma}\right)^2}, \quad (54)$$

$$K = \left(1 + \frac{2}{\gamma}\right)^2 \frac{\sqrt{1 + \frac{3}{2N}}}{1 + \frac{1}{2N} \left(1 - \frac{4}{\gamma}\right)}. \quad (55)$$

We show a comparison of the Luttinger parameter K for the different boundary conditions in the Thomas-Fermi regime and the strong coupling regime in Figure 6. The parameter K varies from infinity to $1 + \frac{1}{4N}$. For weak coupling, K increases more quickly than in the periodic case. In the strong coupling limit, K tends to 1 for both cases.

The density fluctuations are suppressed in the weak coupling limit, while they are enhanced in the strong coupling limit. This can be seen directly from the leading term

of the density expectation value [47]

$$\langle \rho(x) \rangle \approx n \left[1 - \frac{1}{\pi} \left(\frac{\pi}{n2L \left| \sin \frac{2\pi x}{2L} \right|} \right)^K \right] \sin(2\pi n x) \quad (56)$$

with $a \ll x \ll L - a$, where a is the cut-off length to the boundaries. For weak coupling we find $a \approx \frac{1}{n\sqrt{\gamma}}$ while in the strong coupling limit $a \approx \frac{2}{\pi n}$. In the weak coupling regime, the density fluctuations are suppressed due to the coherence of the wave functions. However, in the strong coupling limit, density fluctuations are evident due to the decoherence of the wave functions. These effects can be seen directly from equation (56).

7.2. Local correlation g_2

It is well known that the local correlations in the 1D Bose gas decay algebraically [38, 41]. As for the periodic case, we can calculate the two-body correlation functions through the ground state energy for the hard wall boundary conditions. Using the Hellmann-Feynman theorem, the $g_2(\gamma)$ correlation function is given by [40, 43]

$$g_2(\gamma) = n^2 \frac{\partial}{\partial \gamma} \left(e_0(\gamma) + \frac{1}{N} e_f(\gamma) \right). \quad (57)$$

We thus obtain the correlation function g_2 in the various regions as

$$g_2(\gamma) = \begin{cases} \frac{4\pi^2 n^2}{3\gamma^2 \left(1 + \frac{2}{\gamma}\right)^3} \left(1 + \frac{3}{2N}\right), & \text{for } \gamma > 5 \\ n^2 \left(1 - \frac{2\sqrt{\gamma}}{\pi} + \frac{4}{3N\sqrt{\gamma}}\right), & \text{for } \frac{1}{N^2} \ll \gamma \ll 1 \\ \frac{3}{2}n^2, & \text{for } \gamma \ll \frac{1}{N^2}. \end{cases} \quad (58)$$

These results are to be compared with the periodic case, for which

$$g_2(\gamma) = \begin{cases} \frac{4\pi^2 n^2}{3\gamma^2 \left(1 + \frac{2}{\gamma}\right)^3}, & \text{for } \gamma > 5 \\ n^2 \left(1 - \frac{2\sqrt{\gamma}}{\pi}\right), & \text{for } \frac{1}{N^2} \ll \gamma \ll 1 \\ n^2, & \text{for } \gamma \ll \frac{1}{N^2}. \end{cases} \quad (59)$$

The enhancement of the correlation function g_2 by the hard walls is largest for weak coupling, as can be seen in Figure 7. This is due to backward scattering increasing the probability of two particles scattering in comparison with only forward scattering for the periodic case.

8. Conclusion

We have considered the integrable interacting 1D Bose gas in a hard wall box. The exact Bethe Ansatz solution for the wavefunctions and eigenspectrum has been outlined in Appendix A. The ground state energy, including the bulk and surface energy have been derived from the Bethe equations (5) in different regimes. For N bosons, these are (i) the mean-field regime $\gamma \ll 1/N^2$, where the interaction energy is much smaller than the kinetic energy, (ii) the Thomas-Fermi regime $1/N^2 \ll \gamma \ll 1$, and (iii) the strongly

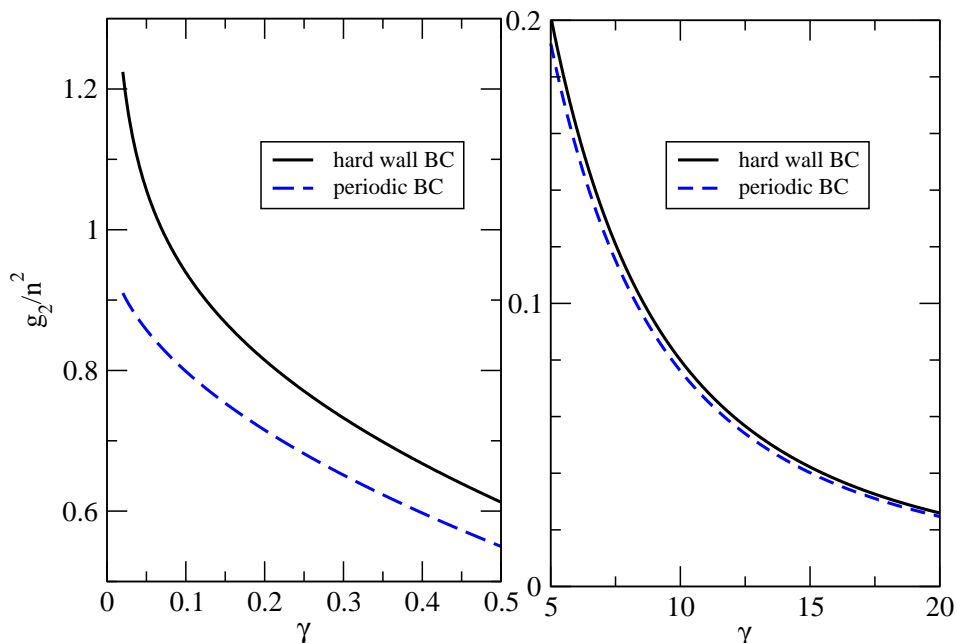


Figure 7. The normalized local correlation function g_2 versus coupling strength γ for (left) weak coupling and (right) strong coupling for $N = 30$ bosons. The enhancement of the correlation function by the hard walls is largest for weak coupling.

interacting Tonks-Girardeau regime $\gamma \gg 1$. These results have been compared with the ground state energy obtained from the continuum Lieb-Liniger-type integral equations in the thermodynamic limit. The latter results, (26)-(28), are in agreement with those found by Gaudin [52]. The emphasis of our approach has been on finite systems and the effects of the hard wall boundary conditions. It is seen that the finite-size results compare well with those from the continuum integral equation, with the exception of the mean-field regime, where the integral equation is not expected to hold.

A connection to the 1D Bose gas trapped by a harmonic potential has also been made. The Luttinger liquid parameters, such as the density stiffness, sound velocity, and the local correlation function g_2 have been calculated from the ground state energy in the various regimes. It is clearly seen that the hard wall boundary conditions have a larger influence on the phase correlations in the weak coupling limit. The enhancement of the Luttinger liquid parameter K strongly suppresses the fluctuation in the ground state density expectation value. The local correlation g_2 is enhanced by the hard wall boundary conditions. A significant effect of the hard wall boundary conditions is that the wave-like properties of the bosons become more pronounced in the weak coupling regime. Significantly, the 1D interacting Bose gas confined in a hard wall box can be experimentally realized. Future experiments, highlighting the subtle interplay between system size and boundary effects in ultracold quantum gases, are eagerly awaited.

Acknowledgments

This work has been supported by the Australian Research Council.

Appendix A. The Bethe Ansatz solution

In this Appendix we present the coordinate Bethe Ansatz solution of the 1D interacting Bose gas with hard wall boundary conditions. The general form of the wavefunction is that of the spin- $\frac{1}{2}$ Heisenberg chain with open boundaries and additional surface terms [61].

First we consider the standard one particle in a box case, $N = 1$, for which the wave function is

$$\Psi(x) = A(k)e^{ikx} - A(-k)e^{-ikx}. \quad (\text{A.1})$$

From the hard wall boundary conditions (2), we have $A(k) = A(-k)$ and $e^{i2kL} = 1$. The energy is $E = k^2$. Thus, up to an overall constant, the wave function is $\Psi(x) = A(k) \sin kx$, with quasi momentum $k = n\pi/L$, where n is a non-zero integer. This describes a trapped particle which has a discrete energy spectrum. If L is infinitely large, the particle becomes free and the energy levels will be continuous.

Next we consider $N = 2$, with wave function Ansatz

$$\begin{aligned} \Psi(x_1, x_2) = & A(k_1, k_2) e^{i(k_1x_1+k_2x_2)} + A(k_2, k_1) e^{i(k_2x_1+k_1x_2)} \\ & - A(-k_1, k_2) e^{i(-k_1x_1+k_2x_2)} - A(-k_2, k_1) e^{i(-k_2x_1+k_1x_2)} \\ & - A(k_1, -k_2) e^{i(k_1x_1-k_2x_2)} - A(k_2, -k_1) e^{i(k_2x_1-k_1x_2)} \\ & + A(-k_1, -k_2) e^{-i(k_1x_1+k_2x_2)} + A(-k_2, -k_1) e^{-i(k_2x_1+k_1x_2)} \end{aligned} \quad (\text{A.2})$$

with the domain $0 \leq x_1 < x_2 \leq L$. For $x_1 \neq x_2$, $H\Psi(x_1, x_2) = (k_1^2 + k_2^2)\Psi(x_1, x_2)$. For $x_1 = x_2$, the consistency condition for the wave function to be continuous is

$$\left(\frac{\partial}{\partial x_2} - \frac{\partial}{\partial x_1} \right) \Psi(x_1, x_2)|_{x_1=x_2} = c\Psi(x_1, x_2) \quad (\text{A.3})$$

which leads to the relations

$$\begin{aligned} A(k_1, k_2) &= \frac{k_1 - k_2 + ic}{k_1 - k_2 - ic} A(k_2, k_1), \\ A(-k_1, k_2) &= \frac{k_1 + k_2 - ic}{k_1 + k_2 + ic} A(k_2, -k_1), \\ A(k_1, -k_2) &= \frac{k_1 + k_2 + ic}{k_1 + k_2 - ic} A(-k_2, k_1), \\ A(-k_1, -k_2) &= \frac{k_1 - k_2 - ic}{k_1 - k_2 + ic} A(-k_2, -k_1), \end{aligned} \quad (\text{A.4})$$

between the coefficients $A(k_{P1}, k_{P2})$. Using the hard wall boundary conditions (2), the unnormalized wave function is

$$\begin{aligned} \Psi(x_1, x_2) = & (k_1 - k_2 + ic)(k_1 + k_2 - ic) e^{i(k_1x_1+k_2x_2)} \\ & + (k_1 - k_2 - ic)(k_1 + k_2 - ic) e^{i(k_2x_1+k_1x_2)} \end{aligned}$$

$$\begin{aligned}
& - (k_1 - k_2 + ic)(k_1 + k_2 - ic) e^{i(-k_1x_1+k_2x_2)} \\
& - (k_1 - k_2 + ic)(k_1 + k_2 + ic) e^{i(k_2x_1-k_1x_2)} \\
& - (k_1 + k_2 + ic)(k_1 - k_2 - ic) e^{i(k_1x_1-k_2x_2)} \\
& - (k_1 - k_2 - ic)(k_1 + k_2 - ic) e^{i(-k_2x_1+k_1x_2)} \\
& + (k_1 - k_2 - ic)(k_1 + k_2 + ic) e^{-i(k_1x_1+k_2x_2)} \\
& + (k_1 - k_2 + ic)(k_1 + k_2 + ic) e^{-i(k_2x_1+k_1x_2)}, \tag{A.5}
\end{aligned}$$

provided that the Bethe equations

$$\begin{aligned}
e^{i2k_1L} &= \frac{(k_1 - k_2 + ic)(k_1 + k_2 + ic)}{(k_1 - k_2 - ic)(k_1 + k_2 - ic)}, \\
e^{i2k_2L} &= \frac{(k_2 - k_1 + ic)(k_2 + k_1 + ic)}{(k_2 - k_1 - ic)(k_2 + k_1 - ic)}, \tag{A.6}
\end{aligned}$$

are satisfied.

Observe that for $c = 0$, the wave function (A.5) reduces to the standing wave $\Psi(x_1, x_2) = \sin k_1x_1 \sin k_2x_2 + \sin k_2x_1 \sin k_1x_2$, with $k_1 = n_1\pi/L$ and $k_2 = n_2\pi/L$ for n_1 and n_2 non-zero integers. When c increases, k_1 and k_2 also increase as if the boson mass increases. The standing wave properties are gradually lost as the interaction becomes stronger.

In a similar way, we can derive the N -particle wave function given in (3). The coefficients are connected to each other via

$$A(\dots, \epsilon_i k_i, \dots, \epsilon_j k_j, \dots) = \frac{\epsilon_i k_i - \epsilon_j k_j + ic}{\epsilon_i k_i - \epsilon_j k_j - ic} A(\dots, \epsilon_j k_j, \dots, \epsilon_i k_i, \dots), \tag{A.7}$$

for $i < j$. Application of the boundary conditions leads to the explicit form of the coefficients given in (4), along with the Bethe equations (2). The wave function is unnormalized.

- [1] Dalfovo F, Pitaevskii L P and Stringari S J 1999 *Rev. Mod. Phys.* **71** 463
- [2] Leggett A J 2001 *Rev. Mod. Phys.* **73** 307
- [3] Cornell E A and Wieman C E 2002 *Rev. Mod. Phys.* **74** 875
- [4] Ketterle W 2002 *Rev. Mod. Phys.* **74** 1131
- [5] Jochim S *et al* 2003 *Science* **302** 2101
- [6] Chin C *et al* 2004 *Science* **305** 1128
- [7] Regal C A, Greiner M and Jin D S 2004 *Phys. Rev. Lett.* **92** 040403
- [8] Görlitz A *et al* 2001 *Phys. Rev. Lett.* **87** 130402
- [9] Olshanii M 1998 *Phys. Rev. Lett.* **81** 938
- [10] Petrov D S, Shlyapnikov G V and Walraven J T M 2000 *Phys. Rev. Lett.* **85** 3745
- [11] Dunjko V, Lorent V and Olshanii M 2001 *Phys. Rev. Lett.* **86** 5413
- [12] Gangardt D M and Shlyapnikov G V 2003 *Phys. Rev. Lett.* **90** 010401
- [13] Tokatly I V 2004 *Phys. Rev. Lett.* **93** 090405
- [14] Girardeau M D, Wright E M and Triscari J M 2001 *Phys. Rev. A* **63** 033601
- [15] Lieb E H, Seiringer R and Yngvason J 2003 *Phys. Rev. Lett.* **91** 150401
- [16] Lieb E H and Liniger W 1963 *Phys. Rev.* **130** 1605
- [17] McGuire J B 1964 *J. Math. Phys.* **5** 622
- [18] Girardeau M 1960 *J. Math. Phys.* **1** 516
- [19] Greiner M *et al* 2002 *Nature* **415** 39
- [20] Paredes B *et al* 2004 *Nature* **429** 277
- [21] Pollet L, Rombouts S M A and Denteneer P J H 2004 *Phys. Rev. Lett.* **93** 210401
- [22] Kinoshita T, Wenger T and Weiss D S 2004 *Science* **305** 1125
- [23] Moritz H, Stöferle T, Köhl M and Esslinger T 2003 *Phys. Rev. Lett.* **91** 250402
- [24] Zhou H Q, Links J, McKenzie R H and Guan X W 2003 *J. Phys. A: Math. Gen.* **36** L113
Links J, Zhou H Q, McKenzie R H and Gould M D 2003 *J. Phys. A: Math. Gen.* **36** R63
Links J and Zhou H Q 2002 *Lett. Math. Phys.* **60** 275
- [25] Haldane F D M 1981 *Phys. Rev. Lett.* **47** 1840
- [26] Mattis D C 1993 *The Many-Body Problem* (World Scientific, Singapore)
- [27] Korepin V E, Izergin A G and Bogoliubov N M 1993 *Quantum Inverse Scattering Method and Correlation Functions* (Cambridge: Cambridge University Press)
- [28] Takahashi M 1999 *Thermodynamics of One-Dimensional Solvable Models* (Cambridge: Cambridge University Press)
- [29] Thacker H B 1981 *Rev. Mod. Phys.* **53** 253
- [30] Paul P and Sutherland B 2000 *Phys. Rev. A* **62** 055601
- [31] Wadati M 2002 *J. Phys. Soc. Jpn* **71** 2657
- [32] Sen D 2003 *J. Phys. A: Math. Gen.* **36** 7517
- [33] Amico L and Korepin V 2004 *Ann. Phys.* **314** 496
- [34] Batchelor M T, Guan X W and McGuire J B 2004 *J. Phys. A: Math. Gen.* **37** L497
Batchelor M T, Guan X W, Dunning C and Links J, arXiv:cond-mat/0412645
- [35] Lieb E H 1963 *Phys. Rev.* **130** 1616
- [36] Yang C N and Yang C P 1969 *J. Math. Phys.* **10** 1115
- [37] Berkovich A and Murthy G J 1988 *J. Phys. A: Math. Gen.* **21** L395
Woyrnarovich F, Eckle H-P and Truong T T 1989 *J. Phys. A: Math. Gen.* **22** 4027
- [38] Gangardt D M and Shlyapnikov G V 2003 *New J. Phys.* **5** 79
Astrakharchik G E and Giorgini S 2003 *Phys. Rev. A* **68** 031602(R)
- [39] Cazalilla M A 2003 *Phys. Rev. A* **67** 053606
- [40] Cazalilla M A 2004 *J. Phys. B: At. Mol. Phys.* **37** S1
- [41] Petrov D S, Gangardt D M and Shlyapnikov G V 2004 *J. Phys. IV France* **116** 5
- [42] Oliva J 1989 *Phys. Rev. B* **39** 4197
- [43] Kheruntsyan K V, Gangardt D M, Drummond P D and Shlyapnikov G V, arXiv:cond-mat/0502438
- [44] Liu X J, Drummond P D and Hu H 2005 *Phys. Rev. Lett.* **94** 136406

- [45] Anfuso F and Eggert S 2003 *Phys. Rev. B* **68** 241301
- [46] Holthaus M 2002 *Phys. Rev. E* **65** 036129
- [47] Cazalilla M A 2002 *Europhys. Lett.* **59** 793
- [48] Hänsel W, Hommelhoff P, Hänsch W and Reichel J 2001 *Nature* **413** 498
- [49] Meyrath T P, Schreck F, Hanssen J L, Chuu C-S and Raizen M G 2005 *Phys. Rev. A* **R71** 041604
- [50] Cheianov V V, Smith H and Zvonarev M B, arXiv:cond-mat/0506609
- [51] Cherny A Y and Brand J, arXiv:cond-mat/0507086
- [52] Gaudin M 1971 *Phys. Rev. A* **4** 386
Gaudin M 1983 *la fonction d'onde de Bethe* (Paris: Masson)
- [53] Forrester P J, Frankel N E, Garoni T M and White N S 2003 *Phys. Rev. A* **67** 043607
Forrester P J, Frankel N E, Garoni T M and White N S 2003 *Commun. Math. Phys.* **238** 257
Forrester P J, Frankel N E and Garoni T M 2003 *J. Math. Phys.* **44** 4157
- [54] Wadati M and Kato G 2001 *J. Phys. Soc. Japan* **70** 1924
- [55] Iida T and Wadati M 2005 *J. Phys. Soc. Japan* **74** 1724
- [56] Dukelsky J, Pittel S and Sierra G 2004 *Rev. Mod. Phys.* **76** 643
- [57] Otake S and Sasaki R 2002 *J. Phys. A: Math. Gen.* **35** 8283
Corrigan E and Sasaki R 2002 *J. Phys. A: Math. Gen.* **35** 7017
Ragnisco O and Sasaki R 2004 *J. Phys. A: Math. Gen.* **37** 469
- [58] Sakmann K, Streltsor A I, Alon O E and Cederbaum L S, arXiv:cond-mat/0505323
- [59] Hamer C J, Quispel G R W and Batchelor M T 1987 *J. Phys. A: Math. Gen.* **20** 5677
Hamer C J and Batchelor M T 1990 *J. Phys. A: Math. Gen.* **23** 761
- [60] Sneddon I N 1966 *Mixed Boundary Value Problems in Potential Theory* (Amsterdam: North-Holland Press)
- [61] Alcaraz F C, Barber M N, Batchelor M T, Baxter R J and Quispel G R W 1987 *J. Phys. A: Math. Gen.* **20** 6397